R. & M. No. 3180
(20,654)
A.R.C. Technical Report

MINISTRY OF AVIATION

AERONAUTICAL RESEARCH COUNCIL
REPORTS AND MEMORANDA

Observations of the Flow over a Two-Dimensional 4 per cent Thick Aerofoil at Transonic Speeds

By B. D. HENSHALL, B.Sc., Ph.D., and R. F. CASH, A.F.R.Ae.S.,
OF THE AERODYNAMICS DIVISION, N.P.L.

LONDON: HER MAJESTY'S STATIONERY OFFICE
1961
EIGHT SHILLINGS NET

Observations of the Flow over a Two-Dimensional 4 per cent Thick Aerofoil at Transonic Speeds

By B. D. HENSHALL, B.Sc., Ph.D., and R. F. CASH, A.F.R.Ae.S.,

OF THE AERODYNAMICS DIVISION, N.P.L.

*Reports and Memoranda No. 3180**

January, 1959

Summary. Flow photographs and detailed pressure distributions for a 4 per cent thick circular-arc biconvex aerofoil at transonic speeds are presented. The results for incidences of 0, 1, 2 and 5 deg are analysed in detail.

2. *Introduction.* In previous reports by the present writers, investigations have been made in the National Physical Laboratory 36 in. × 14 in. High-Speed Wind Tunnel of the flow past a two-dimensional 4 per cent thick circular-arc biconvex aerofoil of 9 in. chord at low subsonic[1], high subsonic[2] and supersonic[3] speeds. The present report describes further tests of the same model with 1/11 area ratio slotted-wall transonic liners forming the 14 in. wide roof and floor of the test section. The incidences investigated were 0, 1, 2 and 5 deg and the tunnel free-stream Mach number was varied from 0·60 to that corresponding to the maximum speed of the tunnel.

Throughout these experiments the boundary layers on the aerofoil were naturally turbulent, and were not subjected to artificial transition methods (*see* Ref. 1 for further details). The Reynolds numbers of the current tests were approximately 3×10^6 based on the aerofoil chord of 9 in. Schlieren photographs of the flow were taken using a graded filter[4] and a spark light source of duration $0 \cdot 2 \times 10^{-6}$ sec.

3. *Experimental Data.* Detailed pressure distributions for incidences of $\alpha = 1$, 2 and 5 deg at various free-stream Mach numbers M_0 are presented in Tables 1, 2 and 3 respectively. These results were plotted and integrated to give the normal-force coefficients and the pitching-moment coefficients; numerical results are given in Table 6. Curves of normal-force coefficient C_N against free-stream Mach number M_0 for incidences of $\alpha = 1$, 2 and 5 deg are given in Fig. 1. Further detailed pressure distributions were obtained at two fixed free-stream Mach numbers of 0·60 and 0·70 for ranges of incidence up to 9 deg; these results are presented in Tables 4 and 5.

From these data, the values of the normal-force coefficients C_N were calculated, and these are plotted against incidence for the two constant Mach numbers in Fig. 2.

* Published with the permission of the Director, National Physical Laboratory.

Typical pressure distributions at various free-stream Mach numbers are shown in Figs. 3, 5 and 7 for incidences of 1, 2 and 5 deg respectively. A corresponding series of schlieren photographs appears as Figs. 4, 6 and 8 respectively. Further schlieren photographs for $\alpha = 0$ deg and a range of free-stream Mach number are given in Fig. 9.

It should be noted that the experimental data have not been corrected for blockage or other tunnel-wall interference effects.

4. *Analysis and Discussion of Results.* Comprehensive accounts of the development of separation and its effects on aerofoils at transonic speeds have been given by Pearcey in Ref. 5 and Holder in Ref. 6. The nomenclature adopted in these papers has been employed in the present context, and a sketch illustrating the typical transonic flow pattern of a sharp-nosed aerofoil is given in Fig. 10. We define p_1 and p_2 as the static pressure just upstream and just downstream of the shock wave, whilst p_{TE} denotes the static pressure at the trailing edge of the aerofoil.

The pressure distributions obtained in this investigation have been analysed and the static-pressure ratio values p_1/H_0, p_2/H_0 and p_{TE}/H_0 have been determined. These quantities are plotted against the free-stream static-pressure ratio p_0/H_0 for $\alpha = 1$, 2 and 5 deg respectively in Figs. 11, 12 and 13.

4.1. *Results for $\alpha = 1$ deg.* Well-defined shocks are present on both upper and lower surfaces at $M_0 = 0 \cdot 943$. The schlieren photographs in Fig. 4 show that the boundary layer has separated at the foot of the upper-surface shock: this separation extends to the trailing edge and is already sufficiently well developed to be slowing up the rearward movement of the upper-surface shock wave relative to that of the lower-surface shock wave as the free-stream Mach number is raised[5]. This results in a slowly decreasing value of the normal-force coefficient C_N with increase in free-stream Mach number; the minimum C_N occurs when the lower-surface shock reaches the trailing edge. As the free-stream Mach number is increased beyond this value, the upper-surface shock accelerates to the trailing edge and causes a corresponding increase of lift on the upper surface together with a small increase in C_N.

A 'frozen' shape of the sonic-range pressure distribution exists on both surfaces at $M_0 = 0 \cdot 997$ and further increase of free-stream Mach number has little effect on the flow pattern as shown by Fig. 3. The normal force on the aerofoil remains constant and thus the normal-force coefficient C_N falls gradually as the free-stream Mach number (and hence $\frac{1}{2}\rho V^2$) is increased.

4.2. *Results for $\alpha = 2$ deg.* The general pattern of the flow development is very similar to that for $\alpha = 1$ deg, except that results are given for Mach numbers low enough to embrace the first occurrence of separation. At $M_0 = 0 \cdot 90$ the upper-surface shock wave, at about 50 per cent chord, is not strong enough to provoke boundary-layer separation. The occurrence of a shock wave on the lower surface as the free-stream Mach number is raised leads[5] to separation of the boundary layer on the upper surface and to a sequence of events similar to that observed for $\alpha = 1$ deg. The curve of normal-force coefficient C_N vs. free-stream Mach number M_0 is very similar to that for $\alpha = 1$ deg (*see* Fig. 1).

In Fig. 5, near $x/c = 0 \cdot 35$, some fluctuations in pressure are shown. These are due to a model imperfection: at high applied loads the joint in the model at $0 \cdot 33$ x/c moved and caused a $0 \cdot 002$ or $0 \cdot 003$ step to appear on the upper surface. The disturbance from this step is clearly shown in the photographs for $M_0 = 0 \cdot 96$ and $M_0 = 0 \cdot 998$ of Fig. 6.

4.3. *Results for* $\alpha = 5$ *deg.* As at the lower incidences, the upper-surface shock moves progressively rearwards with increase in free-stream Mach number; and it is evident from the schlieren photographs of Fig. 8 that at $M_0 = 0 \cdot 774$ and $M_0 = 0 \cdot 805$ the flow separates at the foot of the shock but reattaches again sufficiently far upstream of the trailing edge to leave the flow there relatively undisturbed. As the free-stream Mach number is increased this separation bubble extends slowly in chordwise extent until the pressure rise through the shock fails to restore subsonic flow immediately behind the shock wave; the rate of extension then increases sharply[5]. This occurs just before $M_0 = 0 \cdot 848$. There is an immediate decrease in normal-force coefficient C_N from this point; subsequently the previous flow development pattern described above occurs at this incidence also.

The attached shock wave at the leading edge causes extremely high suction peaks to appear in the (p/H_0) values near the leading edge and at this point the boundary layer is developing in a very favourable compression region: shock-induced separation is extremely unlikely under such favourable conditions where the elementary compression waves are tending to deflect the flow back to the surface.

4.4. *Results for* $\alpha = 0$ *deg.* The variation of trailing-edge pressure ratio $(p/H_0)_{TE}$ with free-stream Mach number at zero incidence is given in Fig. 14; corresponding schlieren photographs appear in Fig. 9. The divergence of the trailing-edge pressure (marked in Fig. 14 by D) is a useful guide to the onset of separation effects such as 'buffeting'. It appears, therefore, that even at zero incidence, separation effects of this kind are likely to occur for the present section. This is not unexpected[6] since the total trailing-edge angle is over 9 deg. The divergence of trailing-edge pressure for $\alpha = 2$ and 5 deg. is shown in Figs. 12 and 13 and cross-plotted on Fig. 1. It is noted that lift divergence and trailing-edge pressure divergence occur simultaneously.

Fig. 15 gives the variation of trailing-edge pressure with increasing incidence at $M_0 = 0 \cdot 60$ and $0 \cdot 70$. Once again divergence of trailing-edge pressure indicates that lift divergence has occurred, and the correlation is illustrated by Figs. 2 and 15.

5. *Conclusions.* The development of the transonic flow past a 4 per cent thick biconvex circular-arc aerofoil has been found to be broadly similar to that described for round-nose aerofoils by Pearcey in Ref. 5. Detailed pressure distributions and flow photographs have been used to illustrate the influence of boundary-layer separation on the transonic flow pattern.

Acknowledgements. Mr. P. J. Peggs assisted in the experimental work and Mrs. N. A. North performed the data reduction.

NOTATION

M_0	Free-stream Mach number (uncorrected)
H_0	Stagnation pressure
p	Local static pressure
C_N	Normal-force coefficient (uncorrected)
c	Aerofoil chord
α	Aerofoil incidence (uncorrected)

Suffices

$_0$	Value of a quantity in the free stream
$_{TE}$	Value of a quantity at the trailing edge of the aerofoil.

REFERENCES

No.	Author	Title, etc.
1	B. D. Henshall and R. F. Cash ..	An experimental investigation of leading-edge flow-separation from a 4 per cent thick two-dimensional biconvex aerofoil. R. & M. 3091. February, 1957.
2	B. D. Henshall and R. F. Cash ..	Observations of the flow past a two-dimensional 4 per cent thick biconvex aerofoil at high subsonic speeds. R. & M. 3092. February, 1957.
3	B. D. Henshall and R. F. Cash ..	Observations of the flow patterns of a two-dimensional 4 per cent thick biconvex aerofoil at $M_0 = 1 \cdot 40$ and $1 \cdot 63$. R. & M. 3093. June, 1957.
4	D. W. Holder and R. J. North ..	Optical methods for examining the flow in high-speed wind tunnels. AGARDograph 23. Part I. November, 1956.
5	H. H. Pearcey	Some effects of shock-induced separation of turbulent boundary layers in transonic flow past aerofoils. (Paper presented at Symposium on boundary-layer effects in aerodynamics at the National Physical Laboratory in March/April, 1955.)
6	D. W. Holder and R. F. Cash ..	Experiments with a two-dimensional aerofoil designed to be free from turbulent boundary-layer separation at small angles of incidence for all Mach numbers. R. & M. 3100. August, 1957.

TABLE 1

$\alpha = 1$ deg

Experimental Results: Detailed Pressure Distributions for 4 per cent Biconvex Aerofoil

	Hole position x/c (per cent)	Values of p/H_0							
		$M_0 =$ 0·943	$M_0 =$ 0·965	$M_0 =$ 0·981	$M_0 =$ 0·997	$M_0 =$ 1·014	$M_0 =$ 1·043	$M_0 =$ 1·068	$M_0 =$ 1·128
Upper Surface	1	0·425	0·429	0·427	0·422	0·420	0·420	0·421	0·419
	2	0·511	0·478	0·473	0·470	0·469	0·466	0·467	0·473
	5	0·568	0·566	0·565	0·564	0·565	0·565	0·563	0·559
	10	0·550	0·546	0·544	0·543	0·541	0·540	0·539	0·534
	16	0·522	0·517	0·515	0·514	0·511	0·509	0·507	0·504
	22	0·500	0·494	0·491	0·488	0·485	0·482	0·479	0·477
	28	0·484	0·477	0·474	0·470	0·467	0·463	0·461	0·458
	34	0·472	0·464	0·460	0·455	0·452	0·447	0·444	0·440
	40	0·463	0·454	0·450	0·445	0·441	0·437	0·433	0·432
	46	0·453	0·444	0·440	0·436	0·432	0·426	0·422	0·416
	52	0·443	0·433	0·428	0·424	0·419	0·413	0·409	0·400
	58	0·433	0·423	0·418	0·412	0·412	0·402	0·397	0·388
	64	0·428	0·417	0·411	0·406	0·402	0·395	0·391	0·380
	70	0·417	—	—	0·394	—	—	—	—
	76	0·408	0·397	0·391	0·386	0·382	0·375	0·371	0·359
	82	0·499	0·386	0·380	0·374	0·370	0·363	0·358	0·345
	88	0·575	0·521	0·376	0·366	0·362	0·354	0·352	0·341
	94	0·603	0·575	0·528	0·362	0·354	0·348	0·344	0·334
	97	0·618	0·588	0·548	0·442	0·353	0·346	0·341	0·331
	100	0·629	0·598	0·565	0·506	0·418	0·406	0·396	0·400
Lower Surface	0·5	0·764	0·759	0·751	0·755	0·752	0·749	0·746	0·742
	1·5	0·731	0·727	0·725	0·723	0·721	0·717	0·714	0·711
	3	0·692	0·687	0·685	0·685	0·681	0·678	0·675	0·673
	6	0·655	0·651	0·649	0·649	0·644	0·640	0·637	0·635
	10	0·627	0·621	0·619	0·617	0·615	0·610	0·607	0·604
	18	0·593	0·581	0·578	0·575	0·572	0·568	0·564	0·559
	26	0·554	0·547	0·543	0·540	0·536	0·531	0·527	0·520
	34	0·528	0·521	0·518	0·515	0·512	0·508	0·504	0·496
	42	0·519	0·504	0·499	0·494	0·492	0·487	0·483	0·474
	50	0·496	0·487	0·481	0·476	0·471	0·466	0·463	0·453
	58	0·478	0·472	0·466	0·461	0·456	0·450	0·446	0·436
	66	0·467	0·455	0·452	0·446	0·441	0·434	0·430	0·421
	73	0·457	0·443	0·440	0·434	0·430	0·423	0·418	0·408
	79	0·470	0·434	0·430	0·424	0·419	0·413	0·409	0·400
	85	0·558	0·420	0·414	0·410	0·406	0·399	0·394	0·384
	91	0·584	0·439	0·422	0·411	0·397	0·391	0·387	0·377
	97	0·608	0·571	0·505	0·414	0·393	0·391	0·380	0·397
	100	0·629	0·598	0·565	0·506	0·418	0·406	0·396	0·400

(80623) A*

TABLE 2

$\alpha = 2$ deg

Experimental Results: Detailed Pressure Distributions for 4 per cent Biconvex Aerofoil

	Hole position x/c (per cent)	Values of p/H_0							
		$M_0 =$ 0·770	$M_0 =$ 0·840	$M_0 =$ 0·900	$M_0 =$ 0·960	$M_0 =$ 1·007	$M_0 =$ 1·035	$M_0 =$ 1·085	$M_0 =$ 1·127
Upper Surface	1	0·250	0·273	0·301	0·331	0·346	0·350	0·356	0·360
	2	0·316	0·323	0·345	0·372	0·387	0·389	0·395	0·399
	5	0·626	0·396	0·407	0·423	0·432	0·434	0·437	0·440
	10	0·617	0·534	0·440	0·448	0·453	0·453	0·454	0·456
	16	0·610	0·574	0·451	0·458	0·460	0·458	0·457	0·460
	22	0·610	0·561	0·435	0·436	0·433	0·431	0·428	0·428
	28	0·608	0·548	0·427	0·424	0·421	0·418	0·414	0·413
	34	0·613	0·553	0·449	0·437	0·429	0·424	0·416	0·411
	40	0·615	0·553	0·415	0·405	0·395	0·391	0·386	0·383
	46	0·613	0·549	0·435	0·416	0·407	0·402	0·396	0·392
	52	0·616	0·554	0·444	0·420	0·405	0·394	0·381	0·372
	58	0·624	0·564	0·540	0·408	0·395	0·390	0·381	0·369
	64	0·630	0·572	0·540	0·401	0·387	0·381	0·372	0·366
	70	0·634	0·578	0·540	0·395	—	—	0·366	0·358
	76	0·645	0·592	0·552	0·383	0·367	0·361	0·354	0·348
	82	0·656	0·606	0·570	0·444	0·353	0·348	0·341	0·335
	88	0·672	0·627	0·593	0·551	0·350	0·344	0·334	0·329
	94	0·690	0·650	0·619	0·582	0·341	0·335	0·326	0·320
	97	0·705	0·669	0·639	0·592	0·362	0·336	0·323	0·317
	100	0·717	0·683	0·653	0·605	0·456	0·405	0·392	0·383
Lower Surface	0·5	0·882	0·858	0·833	0·808	0·795	0·791	0·783	0·779
	1·5	0·841	0·815	0·792	0·768	0·757	0·754	0·747	0·743
	3	0·800	0·772	0·747	0·724	0·713	0·710	0·703	0·700
	6	0·765	0·735	0·707	0·684	0·673	0·668	0·662	0·659
	10	0·740	0·706	0·677	0·652	0·640	0·636	0·629	0·626
	18	0·708	0·670	0·636	0·608	0·595	0·591	0·583	0·579
	26	0·684	0·644	0·607	0·574	0·559	0·554	0·546	0·541
	34	0·674	0·627	0·585	0·546	0·530	0·524	0·517	0·514
	42	0·667	0·618	0·574	0·534	0·519	0·507	0·497	0·491
	50	0·660	0·610	0·563	0·511	0·494	0·492	0·477	0·470
	58	0·659	0·607	0·558	0·497	0·474	0·471	0·462	0·454
	66	0·655	0·602	0·551	0·480	0·459	0·454	0·446	0·438
	73	0·661	0·611	0·563	0·473	0·446	0·440	0·433	0·427
	79	0·664	0·615	0·569	0·483	0·439	0·432	0·423	0·417
	85	0·668	0·621	0·577	0·496	0·422	0·416	0·408	0·402
	91	0·681	0·637	0·599	0·564	0·416	0·408	0·399	0·393
	97	0·700	0·662	0·631	0·586	0·412	0·399	0·390	0·385
	100	0·717	0·683	0·653	0·605	0·456	0·405	0·392	0·383

TABLE 3

$\alpha = 5$ deg

Experimental Results: Detailed Pressure Distributions for 4 per cent Biconvex Aerofoil

	Hole position x/c (per cent)	Values of p/H_0							
		$M_0 =$ 0·774	$M_0 =$ 0·848	$M_0 =$ 0·889	$M_0 =$ 0·918	$M_0 =$ 0·959	$M_0 =$ 0·999	$M_0 =$ 1·022	$M_0 =$ 1·077
Upper Surface	1	0·096	0·113	0·139	0·161	0·185	0·201	0·207	0·216
	2	0·093	0·173	0·202	0·218	0·237	0·249	0·251	0·259
	5	0·227	0·252	0·275	0·287	0·300	0·308	0·312	0·315
	10	0·282	0·293	0·312	0·321	0·332	0·338	0·340	0·341
	16	0·312	0·318	0·329	0·336	0·345	0·349	0·350	0·351
	22	0·448	0·319	0·327	0·332	0·338	0·340	0·341	0·340
	28	0·532	0·324	0·329	0·332	0·336	0·337	0·337	0·335
	34	0·579	0·319	0·322	0·324	0·326	0·327	0·326	0·324
	40	0·608	0·323	0·326	0·327	0·327	0·327	0·327	0·325
	46	0·610	0·313	0·313	0·311	0·310	0·308	0·307	0·304
	52	0·612	0·488	0·300	0·309	0·307	0·305	0·303	0·300
	58	0·616	0·506	0·462	0·302	0·297	0·294	0·292	0·286
	64	0·621	0·519	0·489	0·460	0·289	0·286	0·283	0·278
	70	0·625	0·534	0·496	0·475	0·293	—	—	—
	76	0·636	0·562	0·503	0·478	0·295	0·298	0·297	0·292
	82	0·647	0·580	0·512	0·488	0·456	0·289	0·286	0·280
	88	0·665	0·605	0·526	0·497	0·475	0·302	0·297	0·295
	94	0·684	0·631	0·549	0·514	0·485	0·296	0·290	0·285
	97	0·700	0·635	0·551	0·517	0·487	0·374	0·314	0·305
	100	0·704	0·643	0·557	0·520	0·495	0·427	0·394	0·390
Lower Surface	0·5	0·958	0·972	0·922	0·910	0·896	0·886	0·882	0·878
	1·5	0·918	0·939	0·877	0·865	0·850	0·841	0·838	0·832
	3	0·873	0·896	0·872	0·815	0·799	0·790	0·786	0·781
	6	0·832	0·848	0·783	0·769	0·754	0·744	0·739	0·733
	10	0·801	0·805	0·748	0·734	0·717	0·707	0·702	0·697
	18	0·762	0·771	0·703	0·688	0·669	0·658	0·652	0·646
	26	0·735	0·727	0·670	0·653	0·632	0·620	0·614	0·601
	34	0·714	0·698	0·643	0·625	0·601	0·589	0·582	0·575
	42	0·704	0·674	0·631	0·610	0·586	0·572	0·565	0·558
	50	0·693	0·661	0·615	0·593	0·567	0·551	0·545	0·538
	58	0·687	0·650	0·605	0·580	0·551	0·533	0·527	0·518
	66	0·677	0·641	0·590	0·564	0·526	0·507	0·502	0·498
	73	0·680	0·630	0·591	0·563	0·527	0·495	0·488	0·484
	79	0·679	0·632	0·587	0·556	0·516	0·487	0·479	0·474
	85	0·680	0·631	0·583	0·551	0·499	0·473	0·462	0·455
	91	0·688	0·638	0·586	0·554	0·503	0·470	0·457	0·449
	97	0·699	0·641	0·577	0·544	0·504	0·463	0·453	0·443
	100	0·704	0·643	0·557	0·520	0·495	0·427	0·394	0·390

TABLE 4

$M_0 = 0 \cdot 60$

Experimental Results: Detailed Pressure Distributions for 4 per cent Biconvex Aerofoil

	Hole position x/c (per cent)	Values of p/H_0								
		$\alpha = 1°$	$\alpha = 2°$	$\alpha = 3°$	$\alpha = 4°$	$\alpha = 5°$	$\alpha = 6°$	$\alpha = 7°$	$\alpha = 8°$	$\alpha = 9°$
Upper Surface	1	0·739	0·594	0·590	0·584	0·587	0·598	0·620	0·638	0·651
	2	0·761	0·606	0·583	0·581	0·587	0·600	0·623	0·643	0·658
	5	0·766	0·706	0·589	0·579	0·584	0·598	0·620	0·641	0·657
	10	0·765	0·750	0·661	0·584	0·581	0·593	0·615	0·636	0·652
	16	0·760	0·746	0·735	0·631	0·589	0·593	0·613	0·633	0·650
	22	0·757	0·745	0·741	0·696	0·620	0·600	0·612	0·627	0·641
	28	0·754	0·744	0·738	0·729	0·600	0·620	0·621	0·632	0·644
	34	0·755	0·744	0·740	0·739	0·696	0·644	0·633	0·638	0·645
	40	0·755	0·747	0·741	0·741	0·720	0·668	0·650	0·648	0·652
	46	0·753	0·746	0·741	0·742	0·735	0·692	0·664	0·656	0·655
	52	0·754	0·748	0·744	0·744	0·743	0·715	0·680	0·668	0·664
	58	0·757	0·752	0·748	0·748	0·749	0·727	0·695	0·678	0·670
	64	0·759	0·755	0·751	0·752	0·754	0·740	0·710	0·690	0·678
	70	0·762	0·759	0·756	0·756	0·759	0·751	0·723	0·699	0·686
	76	0·766	0·763	0·761	0·762	0·764	0·758	0·734	0·711	0·689
	82	0·771	0·770	0·768	0·769	0·770	0·762	0·743	0·719	0·699
	88	0·780	0·779	0·777	0·778	0·777	0·771	0·752	0·726	0·705
	94	0·792	0·790	0·789	0·788	0·786	0·778	0·760	0·729	0·714
	97	0·801	0·800	0·798	0·797	0·793	0·781	0·763	0·739	0·719
	100	0·807	0·805	0·807	0·805	0·795	0·781	0·762	0·741	0·723
Lower Surface	0·5	0·882	0·920	0·946	0·964	0·976	0·983	0·986	0·988	0·990
	1·5	0·859	0·891	0·915	0·934	0·947	0·955	0·961	0·964	0·966
	3	0·835	0·862	0·884	0·901	0·914	0·924	0·929	0·933	0·937
	6	0·817	0·838	0·857	0·873	0·886	0·894	0·901	0·905	0·908
	10	0·804	0·822	0·838	0·853	0·864	0·873	0·878	0·882	0·886
	18	0·788	0·803	0·815	0·828	0·838	0·845	0·850	0·853	0·856
	26	0·778	0·790	0·801	0·812	0·821	0·827	0·831	0·834	0·835
	34	0·772	0·782	0·791	0·800	0·808	0·813	0·817	0·818	0·819
	42	0·770	0·778	0·787	0·794	0·801	0·805	0·808	0·808	0·808
	50	0·767	0·775	0·782	0·789	0·794	0·798	0·800	0·799	0·798
	58	0·767	0·774	0·779	0·786	0·790	0·793	0·793	0·792	0·790
	66	0·766	0·771	0·776	0·781	0·785	0·786	0·786	0·783	0·778
	73	0·769	0·774	0·777	0·782	0·785	0·786	0·784	0·783	0·776
	79	0·773	0·777	0·780	0·783	0·786	0·784	0·781	0·775	0·769
	85	0·777	0·779	0·781	0·784	0·786	0·783	0·777	0·770	0·762
	91	0·785	0·787	0·788	0·789	0·789	0·784	0·777	0·767	0·756
	97	0·798	0·798	0·798	0·796	0·793	0·785	0·772	0·757	0·742
	100	0·807	0·805	0·807	0·805	0·795	0·781	0·762	0·741	0·723

TABLE 5

$M = 0{\cdot}70$

Experimental Results: Detailed Pressure Distributions for 4 per cent Biconvex Aerofoil

	Hole position x/c (per cent)	Values of p/H_0								
		$\alpha = 1°$	$\alpha = 2°$	$\alpha = 3°$	$\alpha = 4°$	$\alpha = 5°$	$\alpha = 6°$	$\alpha = 7°$	$\alpha = 8°$	$\alpha = 9°$
Upper Surface	1	0·645	0·461	0·455	0·451	0·464	0·492	0·520	0·544	0·559
	2	0·691	0·490	0·446	0·445	0·465	0·496	0·523	0·548	0·569
	5	0·695	0·602	0·467	0·445	0·463	0·494	0·522	0·548	0·568
	10	0·695	0·673	0·547	0·462	0·460	0·485	0·513	0·538	0·560
	16	0·687	0·668	0·639	0·512	0·475	0·489	0·514	0·539	0·559
	22	0·683	0·667	0·661	0·579	0·504	0·498	0·514	0·533	0·549
	28	0·679	0·665	0·659	0·629	0·542	0·518	0·523	0·537	0·551
	34	0·681	0·668	0·662	0·652	0·581	0·541	0·538	0·544	0·553
	40	0·680	0·669	0·663	0·661	0·621	0·565	0·554	0·555	0·560
	46	0·678	0·668	0·664	0·664	0·640	0·589	0·569	0·564	0·564
	52	0·679	0·671	0·667	0·668	0·657	0·612	0·587	0·576	0·573
	58	0·683	0·677	0·673	0·673	0·669	0·632	0·602	0·587	0·579
	64	0·687	0·681	0·678	0·678	0·679	0·650	0·618	0·599	0·588
	70	0·690	0·686	0·684	0·686	0·688	0·667	0·635	0·610	0·594
	76	0·696	0·693	0·692	0·692	0·695	0·678	0·647	0·621	0·603
	82	0·703	0·702	0·701	0·702	0·703	0·689	0·658	0·632	0·611
	88	0·716	0·715	0·711	0·711	0·712	0·697	0·668	0·640	0·618
	94	0·731	0·730	0·730	0·727	0·722	0·708	0·679	0·651	0·627
	97	0·744	0·743	0·742	0·739	0·730	0·711	0·684	0·656	0·633
	100	0·751	0·750	0·749	0·742	0·730	0·710	0·684	0·660	0·638
Lower Surface	0·5	0·849	0·897	0·929	0·950	0·965	0·973	0·978	0·981	0·985
	1·5	0·820	0·862	0·892	0·913	0·929	0·939	0·945	0·949	0·954
	3	0·790	0·824	0·852	0·873	0·889	0·900	0·906	0·912	0·917
	6	0·766	0·794	0·818	0·837	0·853	0·864	0·871	0·876	0·881
	10	0·749	0·773	0·794	0·811	0·825	0·836	0·843	0·848	0·853
	18	0·727	0·746	0·764	0·778	0·792	0·801	0·807	0·812	0·815
	26	0·713	0·729	0·744	0·758	0·769	0·777	0·782	0·786	0·789
	34	0·704	0·717	0·731	0·742	0·752	0·759	0·763	0·765	0·768
	42	0·701	0·713	0·725	0·735	0·743	0·749	0·752	0·753	0·754
	50	0·697	0·708	0·718	0·726	0·734	0·739	0·740	0·740	0·740
	58	0·697	0·706	0·715	0·722	0·729	0·732	0·731	0·729	0·728
	66	0·695	0·702	0·709	0·715	0·721	0·722	0·720	0·717	0·714
	73	0·702	0·707	0·714	0·718	0·722	0·722	0·719	0·714	0·709
	79	0·705	0·710	0·715	0·718	0·721	0·719	0·714	0·707	0·700
	85	0·710	0·714	0·718	0·720	0·721	0·717	0·709	0·699	0·690
	91	0·723	0·724	0·726	0·727	0·725	0·719	0·708	0·695	0·683
	97	0·740	0·739	0·739	0·736	0·729	0·717	0·698	0·680	0·663
	100	0·751	0·750	0·749	0·742	0·730	0·710	0·684	0·660	0·638

TABLE 6

α (deg)	M_0	C_L	C_m	$\left(\frac{p}{H_0}\right)_{TE}$
0	0·975	0·024	−0·003	0·593
0	0·99	0·016	−0·003	0·544
0	1·0	0·026	−0·003	0·471
0	1·01	0·027	−0·003	0·426
0	1·017	0·026	−0·004	0·414
0	1·023	0·024	−0·004	0·411
0	1·06	0·027	−0·005	0·394
0	1·114	0·026	−0·005	0·385
0	1·14	0·030	−0·005	0·375
1	0·943	0·131	−0·003	0·629
1	0·965	0·127	+0·001	0·598
1	0·981	0·133	−0·005	0·565
1	0·997	0·144	−0·004	0·506
1	1·014	0·159	−0·025	0·418
1	1·028	0·161	−0·027	0·409
1	1·043	0·151	−0·027	0·406
1	1·068	0·150	−0·020	0·396
1	1·095	0·148	−0·023	0·393
1	1·128	0·142	−0·026	0·400
2	0·77	0·242	+0·007	0·717
2	0·84	0·277	0·004	0·683
2	0·90	0·330	+0·005	0·653
2	0·96	0·304	−0·019	0·605
2	0·988	0·297	−0·024	0·536
2	0·997	0·302	−0·032	0·496
2	1·007	0·307	−0·034	0·456
2	1·015	0·311	−0·041	0·411
2	1·035	0·299	−0·036	0·405
2	1·056	0·281	−0·033	0·401
2	1·085	0·272	−0·040	0·392
2	1·127	0·266	−0·040	0·383

α (deg)	M_0	C_L	C_m	$\left(\frac{p}{H_0}\right)_{TE}$
5	0·774	0·641	+0·017	0·704
5	0·805	0·670	+0·011	0·693
5	0·848	0·831	−0·028	0·643
5	0·889	0·739	−0·049	0·557
5	0·918	0·689	−0·056	0·520
5	0·959	0·675	−0·070	0·495
5	0·992	0·691	−0·105	0·453
5	0·999	0·694	−0·109	0·427
5	1·009	0·685	−0·109	0·405
5	1·022	0·668	−0·108	0·394
5	1·046	0·656	−0·109	0·393
5	1·077	0·630	−0·101	0·390
0	0·60	0	0	0·811
1	0·60	0·099	+0·004	0·807
2	0·60	0·192	0·008	0·805
3	0·60	0·319	0·008	0·807
4	0·60	0·423	0·007	0·805
5	0·60	0·532	+0·005	0·795
6	0·60	0·638	−0·014	0·781
7	0·60	0·686	−0·043	0·762
8	0·60	0·711	−0·070	0·741
9	0·60	0·726	−0·083	0·723
10	0·60	0·695	−0·085	0·708
11	0·60	0·682	−0·085	0·697
12	0·60	0·688	−0·090	0·688
0	0·70	0	0	0·754
1	0·70	0·108	+0·005	0·751
2	0·70	0·235	0·004	0·750
3	0·70	0·334	0·010	0·749
4	0·70	0·449	0·006	0·742
5	0·70	0·560	+0·005	0·730
6	0·70	0·661	−0·016	0·710
7	0·70	0·708	−0·047	0·684
8	0·70	0·715	−0·069	0·660
9	0·70	0·713	−0·080	0·638

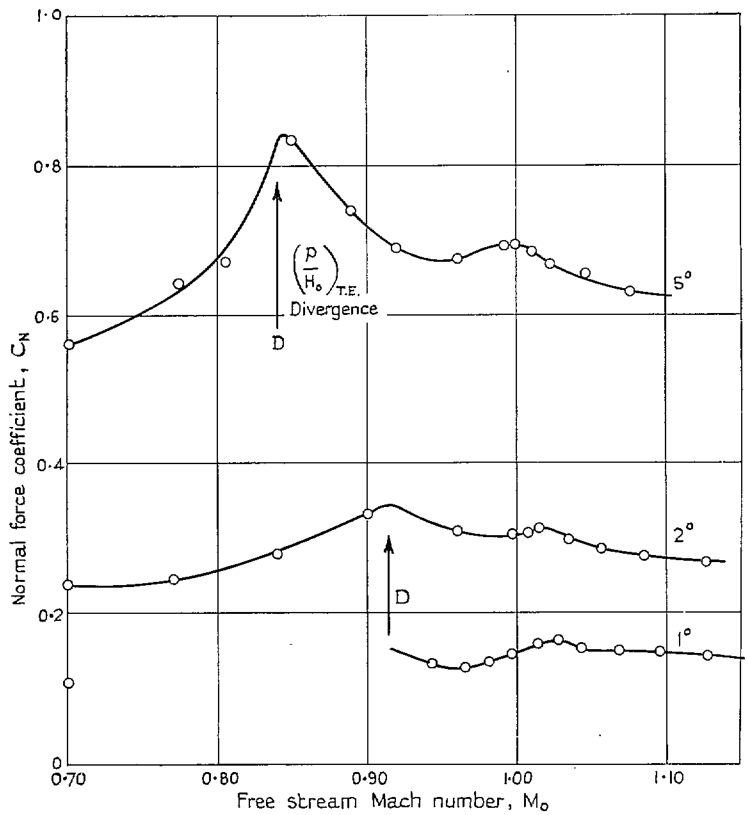

FIG. 1. Variation of normal-force coefficient with free-stream Mach number for a 4 per cent thick two-dimensional biconvex aerofoil at several constant incidences.

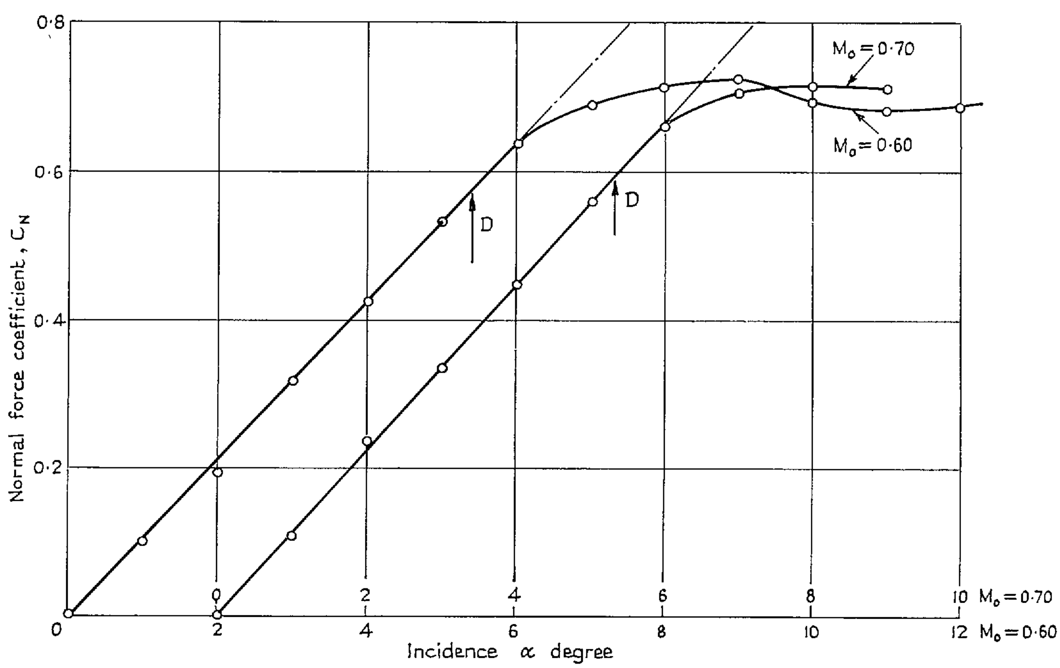

FIG. 2. Variation of normal-force coefficient with incidence for a 4 per cent thick biconvex aerofoil at $M_0 = 0 \cdot 60$ and $0 \cdot 70$.

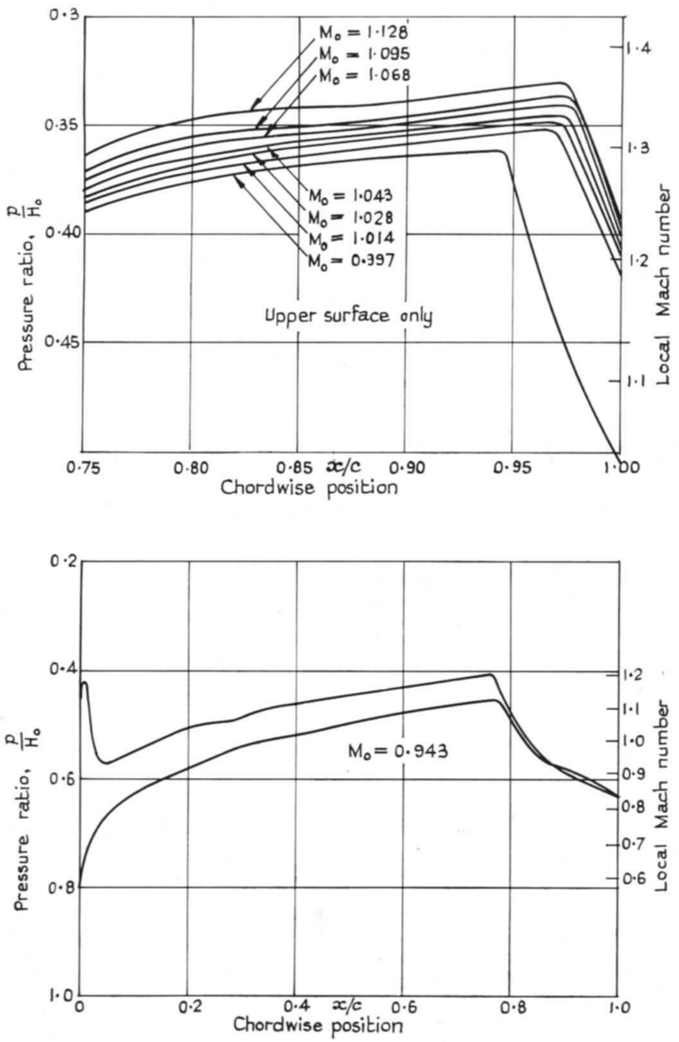

FIG. 3. Pressure distributions for a 4 per cent biconvex aerofoil at $\alpha = 1$ deg.

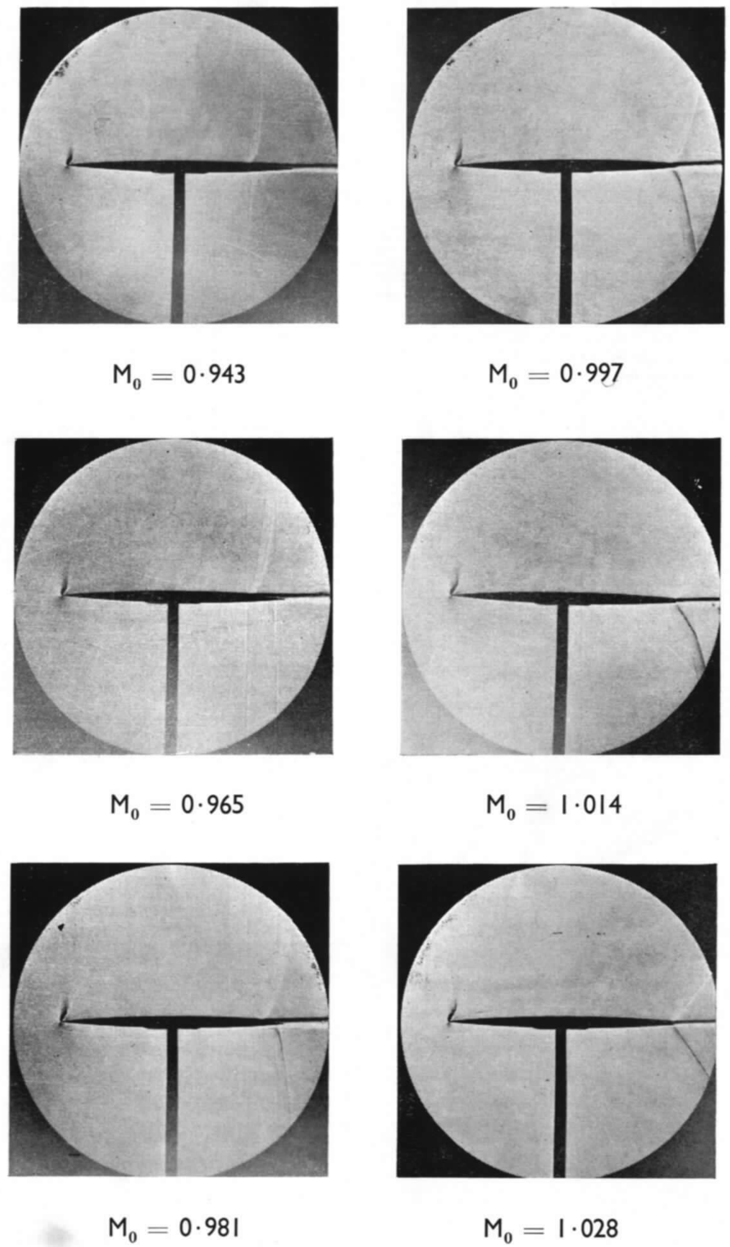

FIG. 4. Schlieren photographs of the flow past a 4 per cent thick biconvex aerofoil at an incidence of 1 deg.

(80623)

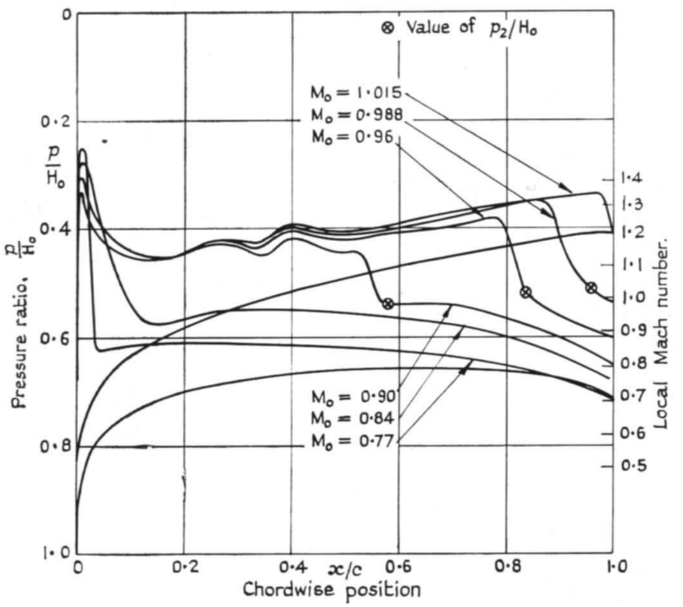

FIG. 5. Pressure distributions for a 4 per cent biconvex aerofoil at $\alpha = 2$ deg.

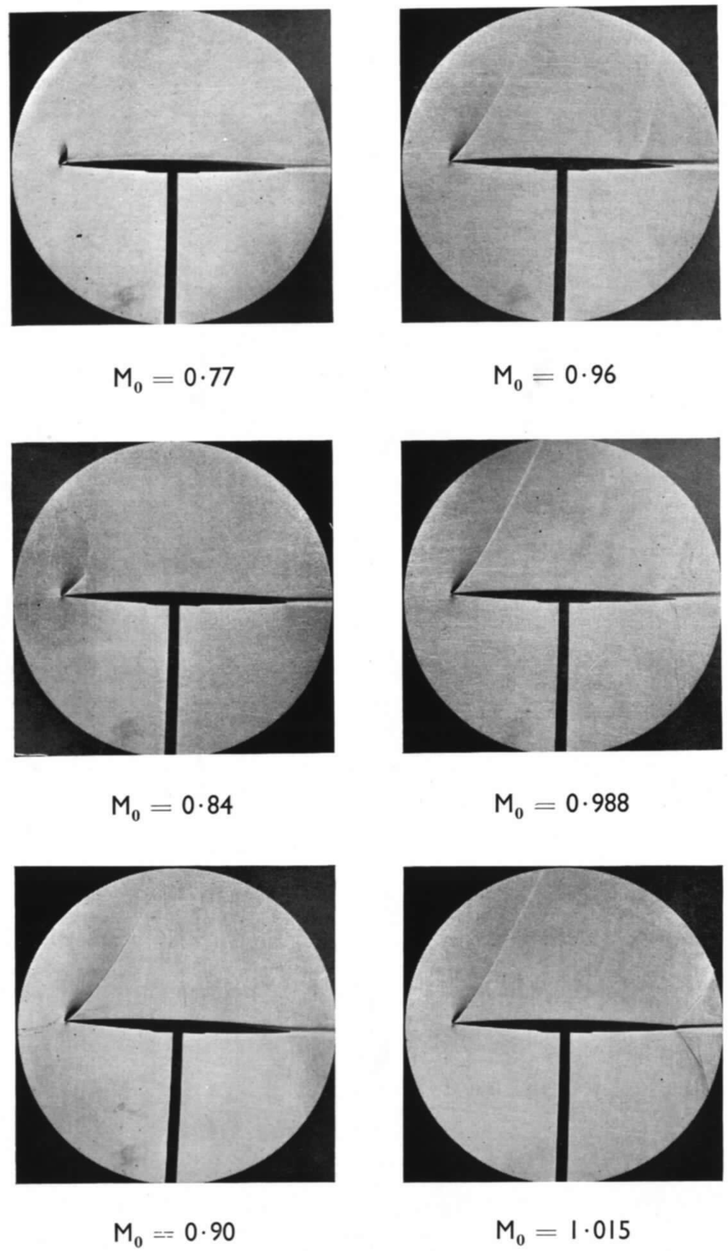

FIG. 6. Schlieren photographs of the flow past a 4 per cent thick biconvex aerofoil at an incidence of 2 deg.

B*

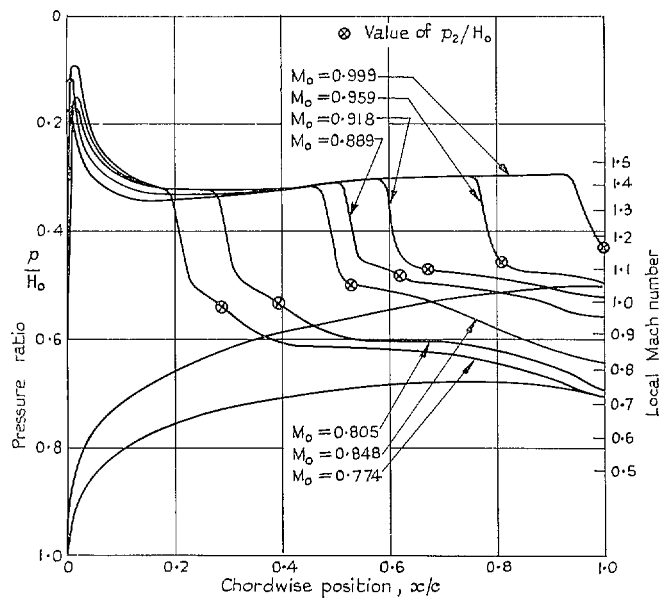

FIG. 7. Pressure distributions for a 4 per cent biconvex aerofoil at α = 5 deg.

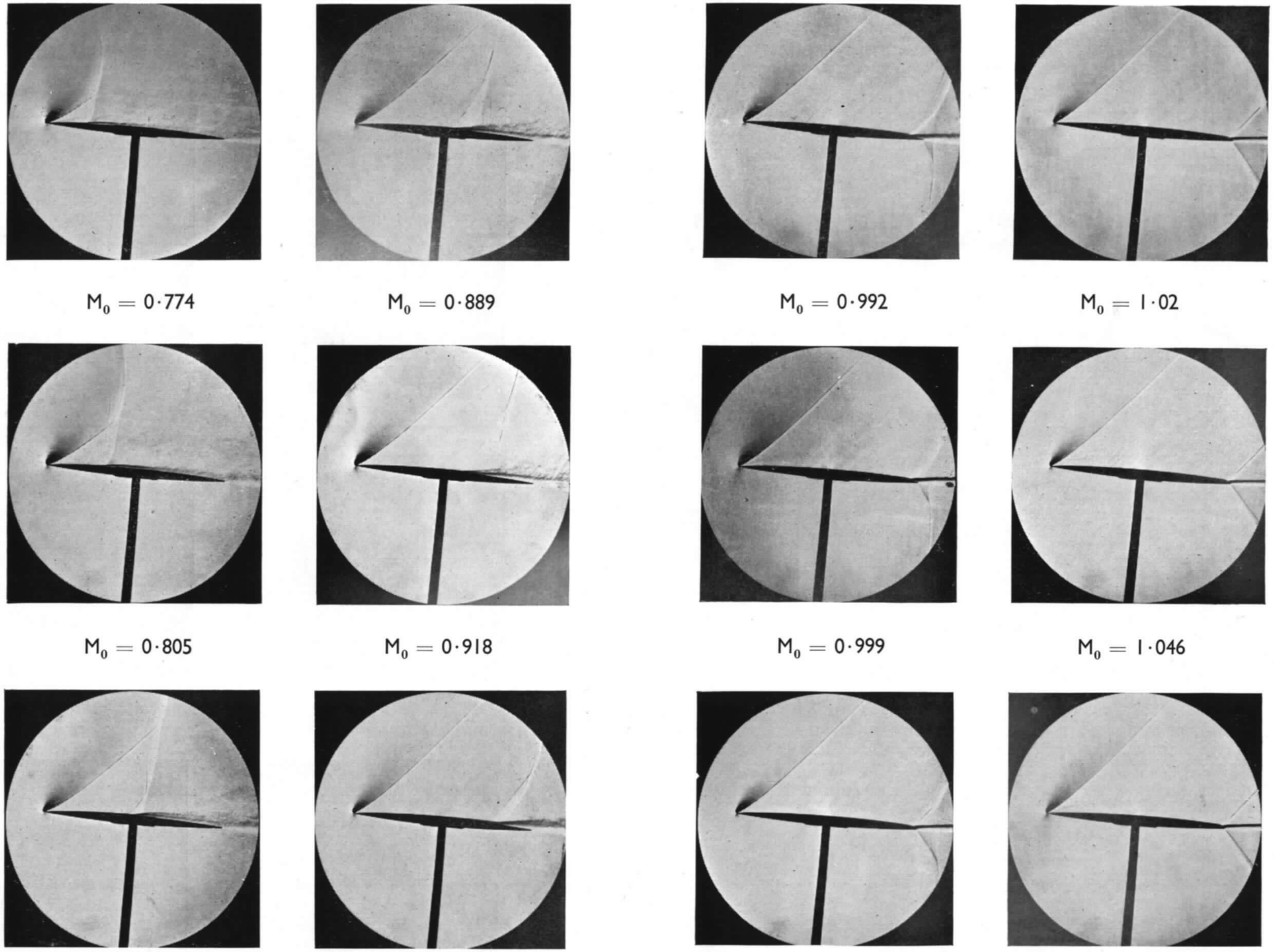

FIG. 8. Schlieren photographs of the flow past a 4 per cent thick biconvex aerofoil at an incidence of 5 deg.

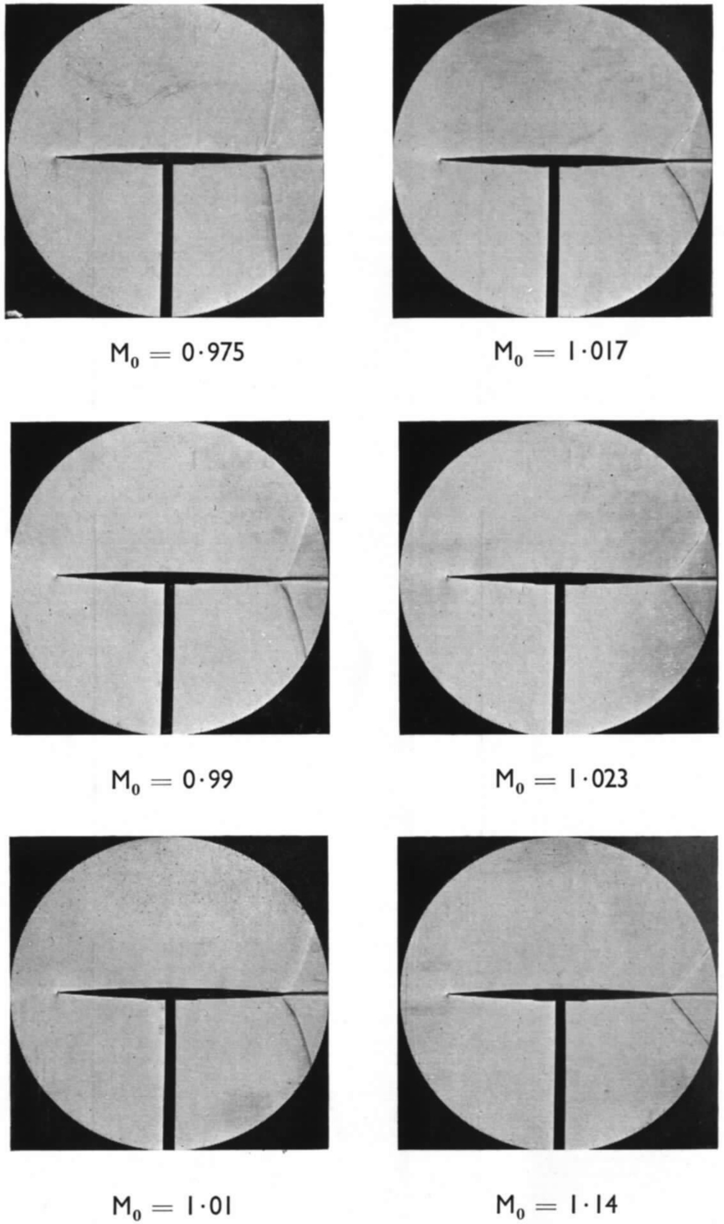

FIG. 9. Schlieren photographs of the flow past a 4 per cent thick biconvex aerofoil at an incidence of 0 deg.

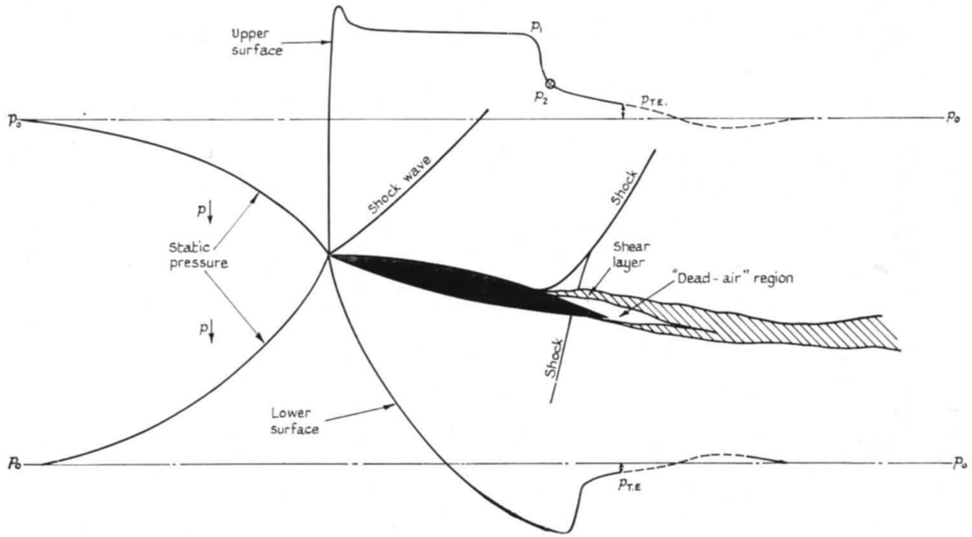

FIG. 10. Sketch of the flow about a sharp-nosed aerofoil at incidence in the presence of shock-induced separation on the upper surface.

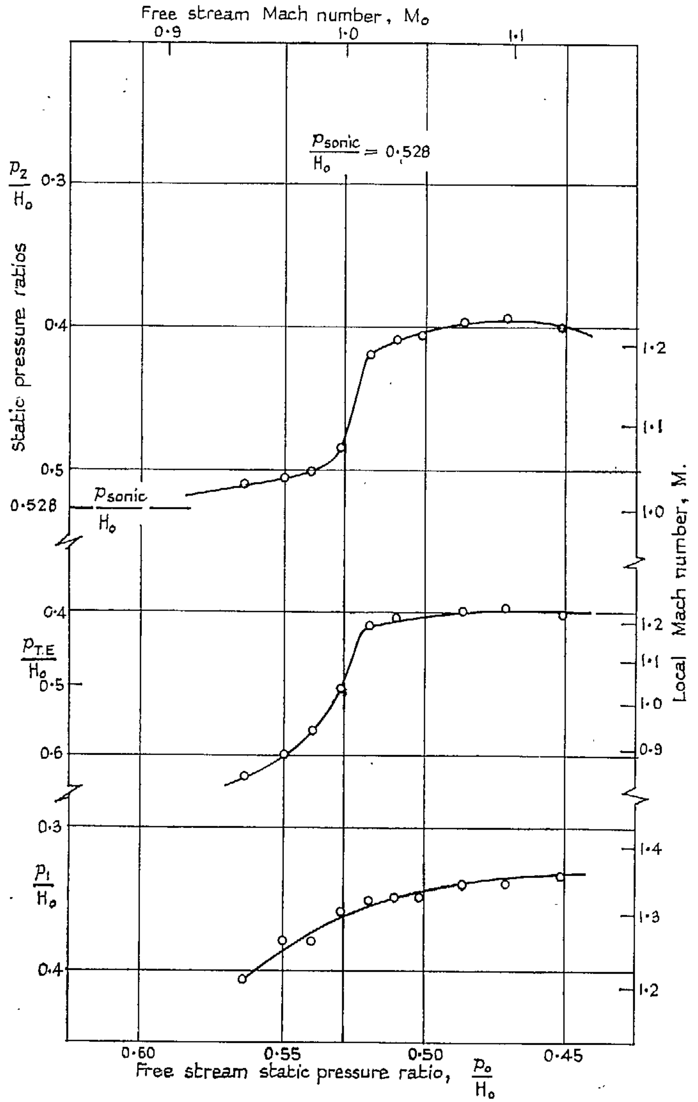

FIG. 11. Variation of p_1/H_0; p_2/H_0 and p_{TE}/H_0 with p_0/H_0 for a 4 per cent thick biconvex aerofoil at transonic speeds and an incidence of 1 deg.

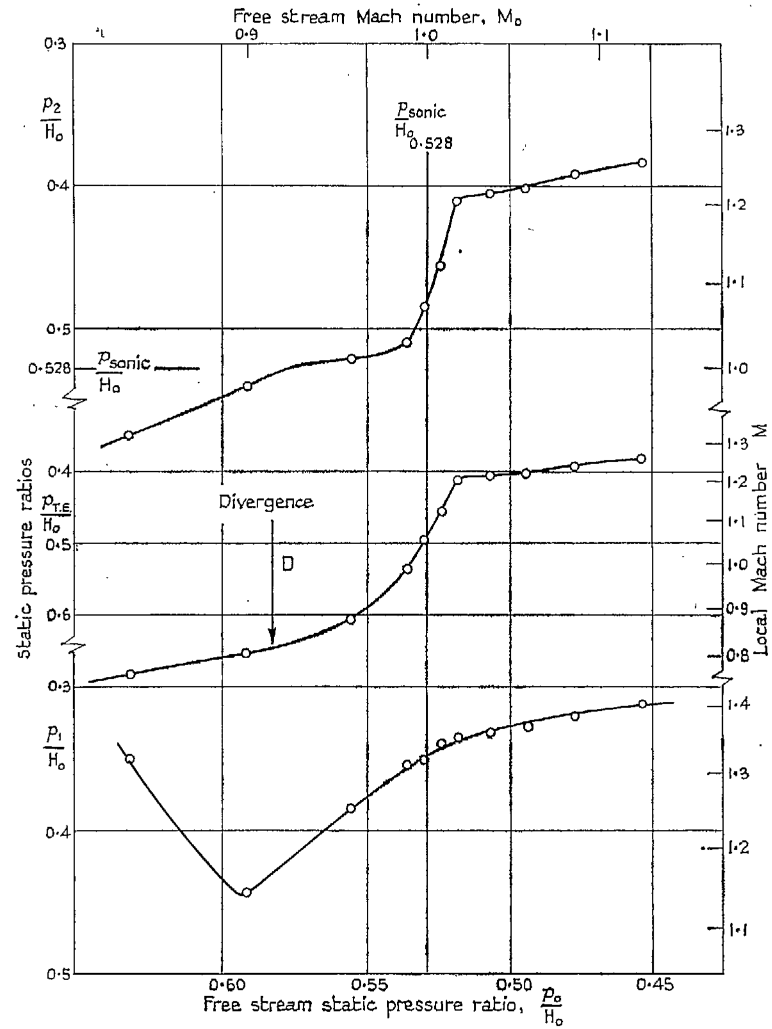

FIG. 12. Variation of p_1/H_0; p_2/H_0 and p_{TE}/H_0 with p_0/H_0 for a 4 per cent thick biconvex aerofoil at transonic speeds and an incidence of 2 deg.

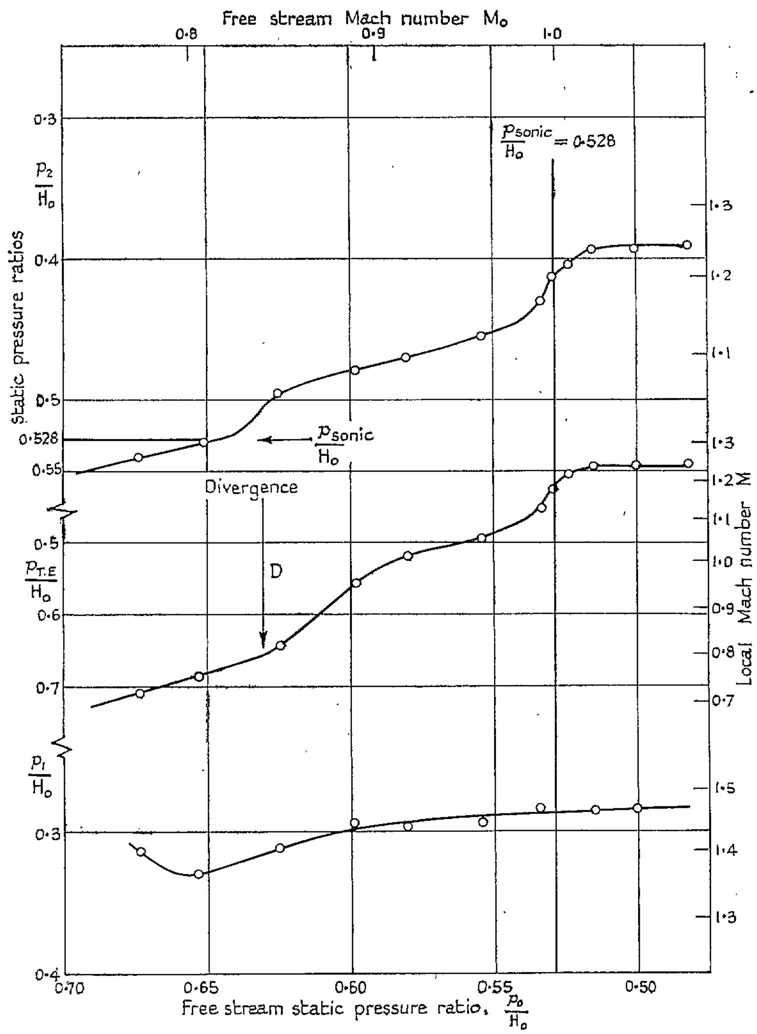

FIG. 13. Variation of p_1/H_0; p_2/H_0 and p_{TE}/H_0 with p_0/H_0 for a 4 per cent thick biconvex aerofoil at transonic speeds and an incidence of 5 deg.

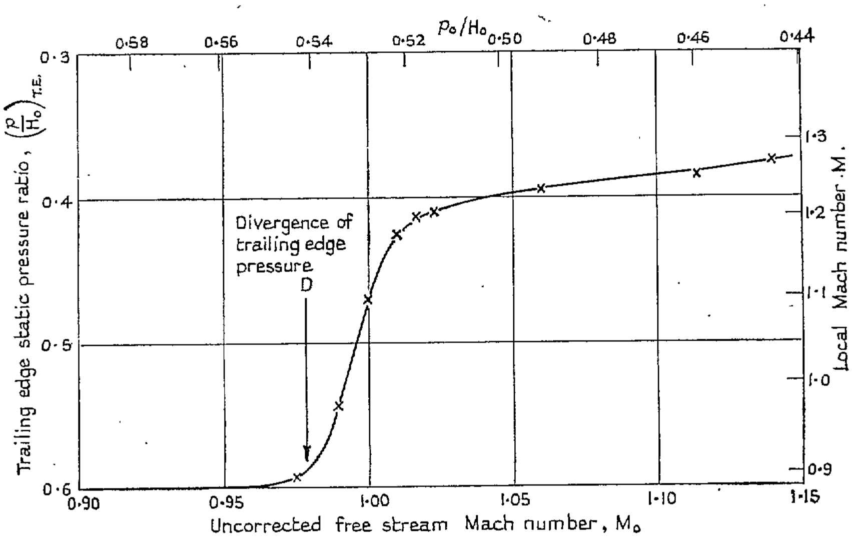

FIG. 14. Variation of $(p/H_0)_{TE}$ with free-stream Mach number for a 4 per cent thick biconvex aerofoil at transonic speeds and zero incidence.

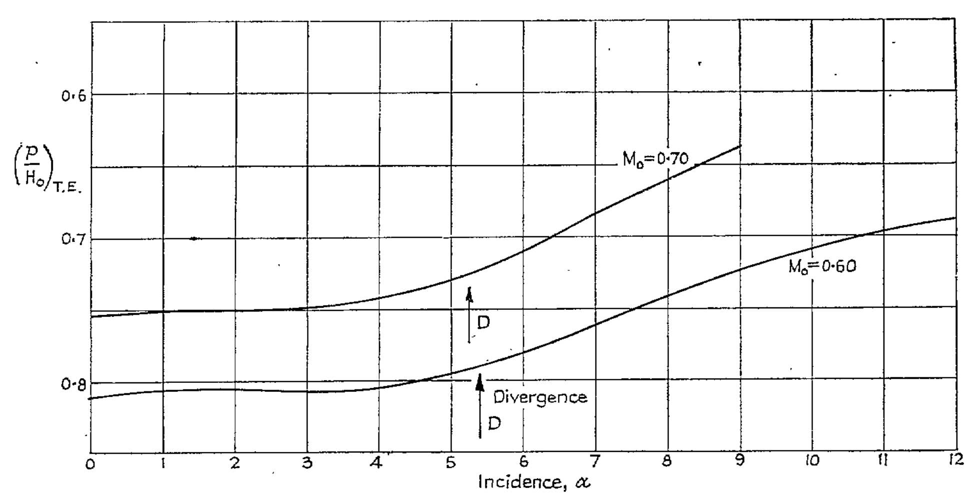

FIG. 15. Variation of trailing-edge pressure coefficient $(p/H_0)_{TE}$ with incidence for a 4 per cent thick biconvex aerofoil at $M_0 = 0{\cdot}60$ and $0{\cdot}70$.

(80623) Wt. 66/991 K.5 1/61 Hw.

Publications of the Aeronautical Research Council

ANNUAL TECHNICAL REPORTS OF THE AERONAUTICAL RESEARCH COUNCIL (BOUND VOLUMES)

1941 Aero and Hydrodynamics, Aerofoils, Airscrews, Engines, Flutter, Stability and Control, Structures. 63*s.* (post 2*s.* 3*d.*)

1942 Vol. I. Aero and Hydrodynamics, Aerofoils, Airscrews, Engines. 75*s.* (post 2*s.* 3*d.*)
Vol. II. Noise, Parachutes, Stability and Control, Structures, Vibration, Wind Tunnels. 47*s.* 6*d.* (post 1*s.* 9*d.*)

1943 Vol. I. Aerodynamics, Aerofoils, Airscrews. 80*s.* (post 2*s.*)
Vol. II. Engines, Flutter, Materials, Parachutes, Performance, Stability and Control, Structures. 90*s.* (post 2*s.* 3*d.*)

1944 Vol. I. Aero and Hydrodynamics, Aerofoils, Aircraft, Airscrews, Controls. 84*s.* (post 2*s.* 6*d.*)
Vol. II. Flutter and Vibration, Materials, Miscellaneous, Navigation, Parachutes, Performance, Plates and Panels, Stability, Structures, Test Equipment, Wind Tunnels. 84*s.* (post 2*s.* 6*d.*)

1945 Vol. I. Aero and Hydrodynamics, Aerofoils. 130*s.* (post 3*s.*)
Vol. II. Aircraft, Airscrews, Controls. 130*s.* (post 3*s.*)
Vol. III. Flutter and Vibration, Instruments, Miscellaneous, Parachutes, Plates and Panels, Propulsion. 130*s.* (post 2*s.* 9*d.*)
Vol. IV. Stability, Structures, Wind Tunnels, Wind Tunnel Technique. 130*s.* (post 2*s.* 9*d.*)

1946 Vol. I. Accidents, Aerodynamics, Aerofoils and Hydrofoils. 168*s.* (post 3*s.* 3*d.*)
Vol. II. Airscrews, Cabin Cooling, Chemical Hazards, Controls, Flames, Flutter, Helicopters, Instruments and Instrumentation, Interference, Jets, Miscellaneous, Parachutes. 168s. (post 2*s.* 9*d.*)

1947 Vol. I. Aerodynamics, Aerofoils, Aircraft. 168*s.* (post 3*s.* 3*d.*)
Vol. II. Airscrews and Rotors, Controls, Flutter, Materials, Miscellaneous, Parachutes, Propulsion, Seaplanes, Stability, Structures, Take-off and Landing. 168*s.* (post 3*s.* 3*d.*)

Special Volumes

Vol. I. Aero and Hydrodynamics, Aerofoils, Controls, Flutter, Kites, Parachutes, Performance, Propulsion, Stability. 126*s.* (post 2*s.* 6*d.*)
Vol. II. Aero and Hydrodynamics, Aerofoils, Airscrews, Controls, Flutter, Materials, Miscellaneous, Parachutes, Propulsion, Stability, Structures. 147*s.* (post 2*s.* 6*d.*)
Vol. III. Aero and Hydrodynamics, Aerofoils, Airscrews, Controls, Flutter, Kites, Miscellaneous, Parachutes, Propulsion, Seaplanes, Stability, Structures, Test Equipment. 189*s.* (post 3*s.* 3*d.*)

Reviews of the Aeronautical Research Council

1939–48 3*s.* (post 5*d.*) 1949–54 5*s.* (post 5*d.*)

Index to all Reports and Memoranda published in the Annual Technical Reports

1909–1947 R. & M. 2600 6*s.* (post 2*d.*)

Indexes to the Reports and Memoranda of the Aeronautical Research Council

Between Nos. 2351–2449	R. & M. No. 2450	2*s.* (post 2*d.*)
Between Nos. 2451–2549	R. & M. No. 2550	2*s.* 6*d.* (post 2*d.*)
Between Nos. 2551–2649	R. & M. No. 2650	2*s.* 6*d.* (post 2*d.*)
Between Nos. 2651–2749	R. & M. No. 2750	2*s.* 6*d.* (post 2*d.*)
Between Nos. 2751–2849	R. & M. No. 2850	2*s.* 6*d.* (post 2*d.*)
Between Nos. 2851–2949	R. & M. No. 2950	3*s.* (post 2*d.*)

HER MAJESTY'S STATIONERY OFFICE

from the addresses overleaf

R. & M. No. 3180

Printed and published by
HER MAJESTY'S STATIONERY OFFICE

To be purchased from
York House, Kingsway, London W.C.2
423 Oxford Street, London W.1
13A Castle Street, Edinburgh 2
109 St. Mary Street, Cardiff
39 King Street, Manchester 2
50 Fairfax Street, Bristol 1
2 Edmund Street, Birmingham 3
80 Chichester Street, Belfast 1
or through any bookseller

Printed in England

R. & M. No. 3180

S.O. Code No. 23-3180